Environmental Engineering and Management Journal *December 2021, Vol. 20, No. 12, 1963-1971*
http://www.eemj.icpm.tuiasi.ro/; http://www.eemj.eu

"Gheorghe Asachi" Technical University of Iasi, Romania

ADSORPTION OF RHODAMINE B ONTO OLIVE POMACE: ISOTHERMS, KINETICS AND INFRARED STUDIES

Imène-Moufida Boukerzaza, Besma Boulhouchet, Brahim Kebabi, Ammar Mennour*

Laboratory Pollution and Water Treatment, Mentouri Brothers University, Constantine, Algeria

Abstract

Olive pomace, an agricultural by-product obtained from an extraction olive oil plant, is tested as a low-cost adsorbent to remove the hazardous rhodamine B dye from aqueous solution. Brunauer-Emmett-Teller (BET) surface area determination and Fourier transform infrared spectroscopic (FTIR) analysis characterized the adsorbent material. The point of zero charge (PZC) was determined (6.3) using a salt addition method. The influence of some operating parameters, namely, initial dye concentration, contact time, solution temperature and solution pH, affecting adsorbent performance is investigated. Maximum adsorption capacity, obtained from the Langmuir isotherm model, was reached in 120 minutes having the value of 86.2 mg g^{-1}. The process is endothermic and the optimum pH was equal to pK_a of rhodamine B (around pH 4). The result of the kinetics study indicated that the adsorption obeys the pseudo-second order model. The FTIR study shows that the main adsorption sites are the surface hydroxyl, carboxyl, and amine functional groups. The results of this study support the assumption that the olive pomace can be used as green adsorbent for rhodamine B in place of some commercial products such activated carbon.

Key words: adsorption, isotherm, kinetics, olive pomace, rhodamine B

Received: October, 2020; Revised final: June, 2021; Accepted: October, 2021; Published in final edited form: December, 2021

1. Introduction

The extensive use of synthetic dyes, especially in the textile industry, and the discharge of untreated colored effluents in the environment causes significant problems. Even in low concentrations, dyes are visible and pose potential human health risks with a genotoxic potential. These contaminants can also negatively affect the hydric environment and the aquatic life (Patel, 2018). Most of the dyes are resistant to biological degradation, and some of them are carcinogenic and mutagenic (Lima et al., 2007). The treatment of colored effluents containing toxic dyes before they are discharged into the environment therefore represents a real technological challenge. There is a huge number of treatment processes such as membrane technology, ion-exchange, chemical precipitation, adsorption, photocatalytic processes, biological and chemical oxidation, electrochemical destruction etc. Despite this fact, searching for low-cost and eco-friendly means of dyes removal is a continuous need. Biosorption is an attractive and feasible method therefore; considerable research has been devoted to developing a multitude of bio-sorbents (Srinivasan and Viraraghavan, 2010). Among bio-sorbing materials, agro-industrial wastes seem to be the most promising (Bharathi and Ramesh, 2013).

Although activated carbon has a high adsorption capacity and has been widely used as an adsorbent for the removal of dyes, agricultural and agricultural by-products have often been used as low-cost adsorbents in wastewater treatment. Agricultural wastes mostly consist of cellulose, hemicellulose, and lignin, which make them a suitable and low-cost alternative to commercial adsorbents. Recently, numerous studies have demonstrated that Agricultural wastes are efficient in the removal of heavy metals and dyes from wastewaters (Guerrero-Coronilla et al., 2019;

* Author to whom all correspondence should be addressed: e-mail: mennourammar@yahoo.fr; Phone: +213 771200504

Imam and Babamale, 2020). Khamparia and Jaspal (2016) studied the adsorptive removing of rhodamine B from aqueous solution using an annual herbaceous plant, (*Argemone Mexicana*) as adsorbent. In another study (Akar et al., 2016) a bio-sorbent obtained from spent biomass of *Pisum sativum* is used to remove reactive dye from aqueous solution. Yapici et al. (2011) used olive pomace to adsorb Tl-201 radionuclide. An adsorption work was carried out for the Ni(II) removal by olive pomace (Nuhoglu and Malkoc, 2009). Martín-Lara et al. (2009) used three different olive oil wastes for heavy metal removal from aqueous solutions. Disperse blue, disperse orange and disperse red were removed from the wastewater using olive pomace as alternative adsorbent material (Rizzi et al., 2017a; 2017b).

Olive pomace (OP), a valuable by-product from olive oil extraction, could be used alternatively as a low-cost natural adsorbent. In the Mediterranean basin, every year, more than 10 million tons of olive pomace are produced and thus occupies a prominent place among the agro-industrial wastes. Although the uses of crude olive pomace are multiple, a large quantity remains without actual application. However, despite numerous papers published on agricultural adsorbents, there is as yet relatively few publications dealing with the use of olive pomace as adsorbent. Olive pomace is constituted from a mixture of pieces of skin, seed, pulp, stone and olive kernel as well as olive oil. It consists of a ligno-cellulosic structure, rich in polyphenolic compounds, uremic acids, and oily residues (Akar et al., 2016). Due to its content of phytotoxic components (phenolic compounds), olive pomace presents major disposal and potentially severe pollution problems.

Rhodamine B (RhB) is a xanthene red dye, highly water-soluble. It is widely used in textile dyeing, paper printing, and leather industries as well as in dental and food stuffs. Rhodamine B causes irritation of the skin, eyes and respiratory tract and is suspected to possess carcinogenic properties and chronic toxicity to humans and animals (EFSA, 2005).

The objective of the present work is to evaluate the adsorptive performance of olive pomace for the removal of RhB dye in aqueous phase. This study reports the influence of some process variables (solution temperature, solution pH, contact time and initial dye concentration) on the RhB adsorption. Kinetics, adsorption isotherms and FTIR spectrophotometry were employed for understanding and discussing the exact nature of adsorption sites and the mechanism of RhB dye sequestration.

2. Material and methods

2.1. Bio-sorbent

The solid waste of oil mill called olive pomace (OP) is a waste acquired, as ground solid particles, in November 2016 from an extraction olive oil plant located in El-Milia in the north-east of Algeria. Raw OP was first washed three times with warm distilled water for removing soluble constituents and oven-dried at 75°C for 48 h. Then, the OP is ground to a fine powder using mortar and pestle. The obtained powder is abundantly washed with demineralized water until it gives colorless filtered water. The washed powder was placed in an oven (75°C) for drying to obtain a constant weight. Finally, it is sieved to 0.15 – 0.25 mm particle size and stored in desiccators until its use.

2.2. Preparation and analysis of RhB solutions

The basic dye rhodamine B ($C_{28}H_{31}ClN_2O_3$, HPLC grade, Mr 479.01 g mol^{-1}, maximum absorption wavelength 555 nm), was purchased from Sigma-Aldrich Corporation. Its chemical structure is shown in Fig. 1. A stock solution of RhB in deionized water (1000 mg L^{-1}) was prepared. Experimental solutions of desired concentrations, varying between 100 and 700 mg L^{-1}, were prepared from stock solution by successive dilutions with deionized water.

The pH of solutions was adjusted by adding 0.1M HCl or 0.1M NaOH, which were purchased from Fluka. The pH was measured using a handheld pH-meter (WTW, PH 330i, Germany).

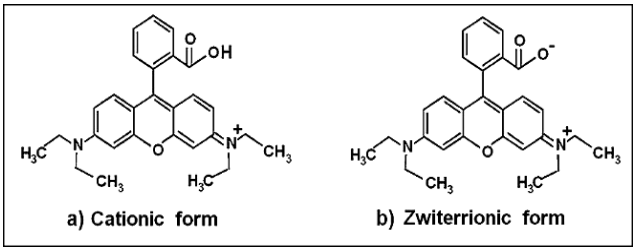

Fig. 1. Molecular form of RhB (cationic and zwitterionic forms)

2.3. Olive pomace characteristics

2.3.1. Determination of point of charge zero

The pH corresponding to the point of zero charge (pH_{pzc}) of OP was determined by the salt addition method. In a series of reaction vessels, 50 ml $NaNO_3$ (0.1M) and 100 mg of adsorbent are mixed. The initial pH (pH_i) of each was then adjusted to a precise value from 2 to 12 using either nitric acid (0.1 M) or sodium hydroxide (0.1 M). The suspensions then were agitated at 120 rpm for 24h and their final pH were measured. The difference between final and initial pH (ΔpH) as a function of pH is plotted and the initial pH at which ΔpH is zero was taken to be the pH_{pzc} (Elisee et al., 2018).

2.3.2. FTIR analysis

The objective of this section is to characterize the raw material and to identify the functional groups which participate in the bonding between RhB species and OP surface after adsorption. FTIR spectra were recorded using a Bruker Tensor 27 instrument (Bruker Optics, Germany). The spectra were collected through the wavenumber range of 900 to 4000 cm^{-1}, with a resolution of 2 cm^{-1} for 32 scans.

2.3.3. N_2 adsorption-desorption at 77 K

Specific surface area based on nitrogen adsorption and desorption isotherms were measured at 77K using the TriStar II 3020 system (Micromeritics Instrument Corporation, USA). The weight of the sample was 0.35 g. The sample was degassed under vacuum at 100°C for 2 h before nitrogen sorption measurement. The specific surface area (m^2g^{-1}) was calculated using the Brunauer, Emmett, and Teller (BET) theory.

2.4. Adsorption procedure

Adsorption and kinetics experiments are conducted by the Batch adsorption method. An accurately weighed quantity of adsorbent is added to a certain volume of RhB dye solution (generally 100 mL) at a known initial concentration and pH. The suspension is stirred at 200 rpm for a chosen time (contact time) and then centrifuged. The supernatant was analyzed using an ultraviolet-visible spectrophotometer (Shimadzu UV-1601PC) at a wavelength, λ_{max}, of 555 nm. The amounts of RhB adsorbed at equilibrium were determined, as the difference between the initial RhB concentration and the one in the supernatant, as follows (Eq. 1):

$$Qe = (C_0 - C_e)V/m \quad (1)$$

where: Q_e is the mass of RhB adsorbed at equilibrium on OP (mg g^{-1}); V is the volume of the RhB solution (L); m is the mass of the adsorbent (g); C_0 and C_e are the initial and equilibrium RhB concentrations (mg L^{-1}) respectively.

The effects of some process variables on the RhB adsorption such as initial dye concentration, contact time, pH and temperature were investigated.

The sorption kinetics experiments were performed by shaking 3g of the adsorbent with 1000 mL of RhB solution (300, 500 and 700 mg L^{-1}). At selected time intervals, 10 mL aliquots of suspension were withdrawn and filtered for spectrophotometric determination of the dye concentration left in the solution. The residual concentrations of RhB were similarly measured.

All experiments were done in triplicate and average values were reported.

2.4. Isotherm modelling

The adsorption equilibrium data were tested against two adsorption isotherm models, namely Langmuir and Freundlich isotherms, respectively expressed with the following equation:

Langmuir equation (Eq. 2):

$$Q_e = Q_m K_L C_e/(1 + K_L C_e) \quad (2)$$

The linearized form of this equation is expressed as (Eq. 3):

$$1/Q_e = (1/Q_m K_L)(1/C_e) + (1/Q_m) \quad (3)$$

Freundlich equation (Eq. 4):

$$Q_e = K_F C_e^{1/n} \quad (4)$$

The linear form of this equation is (Eq. 5):

$$\log Q_e = \log K_F + 1/n \log C_e \quad (5)$$

where: Q_m is the sorbed amount at saturation; K_L (L mg^{-1}) is the Langmuir isotherm constant; K_F (mg g^{-1}) and n are the Freundlich adsorption constants.

2.5. Kinetic analyses of RhB sorption onto OP

The kinetics models of RhB adsorption on the OP were analyzed using pseudo-first order, pseudo-second order, Elovich equation and intraparticle diffusion models. These models are respectively expressed based on the following equations Eqs (6–9):

$$\log(Q_e - Q_t) = \log Q_e - K_1 t/2.303 \quad (6)$$

$$t/Q_t = (1/K_2 Q_e^2) + (t/Q_e) \quad (7)$$

$$Q_t = (1/\beta)\ln \alpha\beta + (1/\beta)\ln t \quad (8)$$

$$Q_e = K_p t^{1/2} + C \quad (9)$$

where: Q_t (mg g^{-1}) is the amount of pollutant adsorbed at time t (min); K_1 is the rate constant of pseudo first-order sorption (L min^{-1}); K_2 is the pseudo-second order rate constant of adsorption; α is the initial adsorption rate (mg $g^{-1}h^{-1}$); β is the desorption constant (g mg^{-1}); C is the intercept, and K_p is the intraparticle diffusion rate constant in mg/g $h^{1/2}$.

3. Results and discussion

3.1. Adsorbent characterization

3.1.1. FTIR

The FTIR spectrum of OP obtained in this study is very close to those reported in several previous studies (Martín-Lara et al., 2008; Pagnanelli et al., 2003; Rizzi et al., 2017a; Yapici et al., 2011) and shows the presence of various functional groups on the surface of the adsorbent. It is noteworthy, however, that the overlapping of bands in the spectrum causes difficulty in band assignment:

- The broad peak at 3340 cm^{-1} can be attributed to the overlap of amino groups and hydroxyl stretching vibrations (Blázquez et al., 2009; Rizzi et al., 2017a; Yapici et al., 2011).
- The peaks at 2925 and 2854 cm^{-1} are due to C−H stretching vibrations (Rizzi et al., 2017a).
- The peaks on 1745 cm^{-1}can be assigned to C=O stretching vibration of carboxylic groups (Yapici et al., 2011) but also can correspond to the stretching vibrations of the carbonyl groups from esters (Martín-Lara et al., 2009).

The peak on 1650 cm^{-1} is assigned to bending mode (δ) of absorbed H_2O and/or of COO^-C=O, and

C–N peptidic bond of proteins (Martín-Lara et al., 2009; Nuhoglu and Malkoc, 2009; Yapici et al., 2011).

- The peaks at 1592, 1540 and 1520 cm^{-1} can be attributed to Secondary amine group (Rizzi et al., 2017a; Yapici et al., 2011).
- The peaks at 1465, 1418, 1378 and 1337 cm^{-1} can be attributed to bending vibration of O–H, related to hydroxyl groups present in lignin, hemicellulose, and cellulose (Martín-Lara et al., 2009).
- The peak at 1275 cm^{-1} can be attributed to $–SO_3$ stretching (Yapici et al., 2011).
- The peak at 1507 cm^{-1} is due to the aromatic ring C–C stretching.
- The peaks at 1316, 1241 cm^{-1} and 1164 cm^{-1} can be due to deformation vibration of C=O of carboxylic groups, stretching vibration of OH of phenols or C–O stretching of ether groups (Martín-Lara et al., 2009; Rizzi et al., 2017a).
- The broad bands at 1120–1000 cm^{-1} represented the characteristic C–O–C and OH vibrations of polysaccharides and, among them, of cellulose (Blázquez et al., 2009; Rizzi et al., 2017a).

The IR spectrum of the OP shows the presence of O–H, COOH, C=O, C–N, C–H, $–NH_2$ and S–OH as functional groups. The diversity of these functional groups indicated the complex nature of the bio-sorbent studied.

3.1.2. pH point of Zero Charge (pHpzc)

The PZC of the OP adsorbent is 6.3. This means its surface is positively charged at pH below 6.3, and negatively at a pH above 6.3.

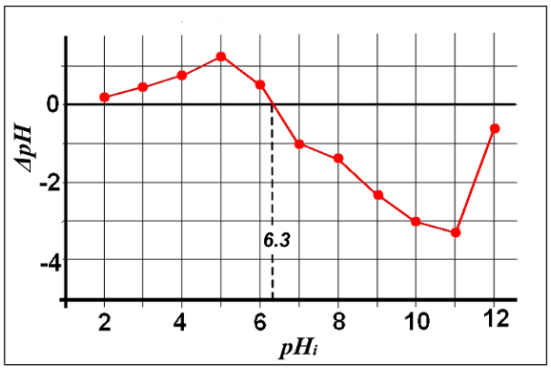

Fig. 2. Determination of pH_{PZC} of OP

3.1.3. Surface Area

As reported previously in the literature (Inyinbor et al., 2015) in general, the agricultural wastes have a low surface area. Not surprisingly, the surface area of OP is found to be as low as 0.968 m^2g^{-1} before RhB adsorption. Therefore, it is theoretically expected that the dye adsorption is likely to be a chemisorption and will be controlled by functional groups interaction.

After the RhB adsorption, it was found that the surface area of OP is 0.936 m^2g^{-1}. Adsorption decreased the BET surface area of OP. This typique decrease is probably due to the clogging of some pores of the adsorbent by the adsorbed species. Similar results have been observed elsewhere (Aboukaïs et al., 2012; Ospina et al., 2015)

3.2. Effect of solution pH

Preliminary investigations showed that the adsorption equilibrium is attained in 120 min, therefore, to ensure that equilibrium has been fully achieved, a contact time of 180 min is employed. Initial RhB concentrations of 300 mg L^{-1}, 500 mg L^{-1} and 700 mg L^{-1}, an OP concentration of 3 g L^{-1} and room temperature (22 ± 1°C) were used.

In this study, RhB uptake was investigated over a wide range of initial pH values, from pH 2.0 to pH 10.0. From the results shown in Fig. 3, it appears that the adsorption capacity of OP is significantly dependent on the solution pH. It can be seen that the optimum initial pH for the dye adsorption is about pH 4.0. An increase or decrease in this solution pH results in a drastic decrease in the amounts of the RhB retained by the adsorbent.

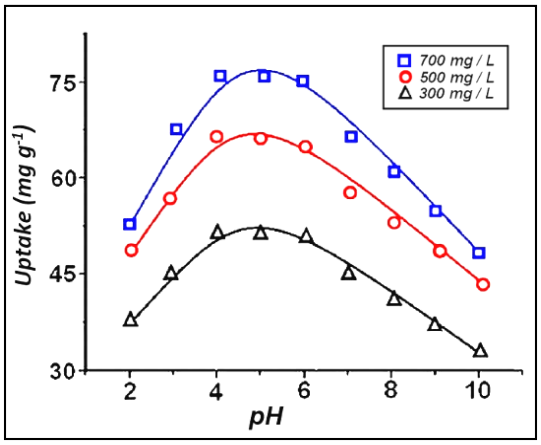

Fig. 3. Effects of pH on RhB adsorption onto olive pomace at 22°C and various initial concentrations of RhB

This pH dependent adsorption could be explained based on two main factors: first the zero point of charge (pH_{pzc}) of the adsorbent and second the form of the dye molecule. Indeed, the pH variation altered surface properties of the sorbent and results in the formation of different ionic forms of the dye (Isa et al., 2007).

The surface charge of the adsorbent and the form of the adsorbate can both play a key role in adsorption (Sergeeva and Sobolev, 2018). The OP surface charge is modified by the protonation/deprotonation of the surface chemical groups and RhB, with pka of 3.7, can exist as cationic or zwitterionic forms (Inyinbor et al., 2016). When the solution pH is lower than 3.7, the RhB molecule has the cationic form (Fig. 1a) and the OP surface is positively charged. At pH greater than that of RhB pka the aromatic carboxyl group gets ionized giving rise to the dipolar form of RhB known as Zwitterions (Fig. 1b). The high capacity of dye removal on OP at pH 4 was, probably, due to the change in sorbent surface character. The negatively charged dyes in solution are

electrostatically attracted by the positively charged surface of the sorbent. With increasing pH levels, the number of positively charged groups of OP decreased significantly, which results in a decreased adsorption of anionic dyes. However, at pH 4 or higher values, the carboxylic side chain of RhB lose a proton and becomes negatively charged (Fig. 1). Due to the electrostatic interactions among the ion-paired molecules of RhB in their zwitterionic form, polymerization of RhB occurs as a consequence of an aggregation process (Kooh et al., 2016a; Venkatraman et al., 2012). The observed sharp decrease in adsorption efficiency, when the pH is higher than 4, can be attributed to the formation of larger RhB species (dimer, trimer, etc.) unable to enter into the pore structure of the surface adsorbent.

When pH decreased from 4.0 to 2.0 the electrostatic repulsion between cationic RhB and positively charged OP leads to the decreased of adsorption. Similar observations have been made earlier (Bhattacharyya et al., 2014; Hou et al., 2011).

3.3. Effect of temperature

The adsorption capacity of OP was evaluated at 278 K, 295 K, and 313 K. By comparing the adsorption isotherms obtained at this different temperature (Fig. 4) one can observe that increasing temperature increases the efficiency of adsorption. At 278K the maximum adsorption (Q_{mexp}) is 60.5 mg g^{-1}, it is 79.8 mg g^{-1} at 295 K while at 313 K it equals to 86.2 mg g^{-1}. This behavior is an indication that the bonding of RhB onto OP is endothermic.

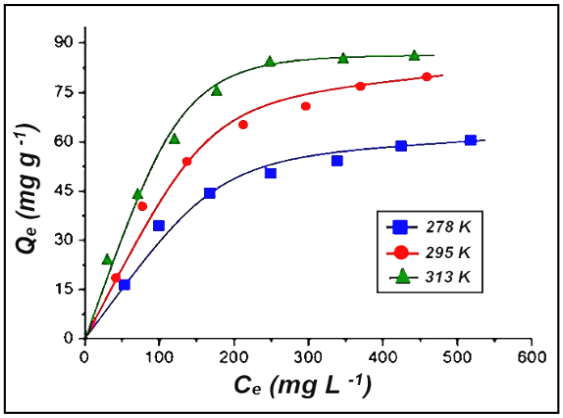

Fig. 4. Adsorption isotherms of RhB on the olive pomace

3.4. Analysis of isotherm data

The adsorption experiments were carried out by a batch method. Adsorption isotherms are created by adding 0.3g of OP to 100 mL of a stock solution of RhB in a closed vessel kept in a thermostatic environment. After shaking the sample for 180 min (200 rpm shaking speed on a shaking table), the suspension is centrifuged at 5000 rpm for 30 min and the supernatant is then pipetted and analyzed to determine the final concentration of RhB. Fig. 4 shows the plot of the adsorbed mass of RhB (Q_e) as a function of its equilibrium concentration in solution (C_e) at a constant temperature. The curves provide an estimation of the adsorption capacity of the adsorbent. It is observed an increase of the adsorption uptake with increasing initial dye concentration. The high initial concentration of RhB means a high number of RhB molecules vying for adsorption sites, hence higher sorption capacity was obtained at higher initial concentrations (Banerjee and Chattopadhyaya, 2017). Fig. 4 revealed that, at the lower analyte concentrations (C_e < 200 mg L^{-1}), the amount of RhB retained on the OP is directly proportional to the amount remained in the bulk solution.

Moreover, this figure shows, at the upper analyte concentrations (C_e > 200 mg L^{-1}), the equilibrium RhB sorption capacity gradually approached a plateau after which the amount of dye adsorbed was negligible as surface binding sites were saturated. This plateau would represent the maximum experimental uptake capacity Q_{mexp} of the adsorbent for RhB at various temperature.

Two well-known isotherm models (Langmuir and Freundlich) were employed to describe equilibrium between adsorbed molecules on the solid and species in solution at different temperatures (278, 295, 313 K). Generally, to estimate the parameters of adsorption isotherms, a linear least squares method and linear coefficients of determination (R^2) are preferred (Crini et al., 2019; Zhao et al., 2021). Table 1 shows the two isotherm models used, together with all the parameters and R^2 values obtained from experimental data.

Table 1. Langmuir and Freundlich parameters for adsorption of RhB on olive pomace

Models	***Parameters***	***278 K***	***295 K***	***313 K***
Langmuir	K_L ($L\ mg^{-1}$)	0.0092	0.0096	0.011
	Q_m ($mg\ g^{-1}$)	72.8	95	106
	R^2	0.997	0.99	0.99
Freundlich	K_f ($mg\ g^{-1}$)	3.035	6.230	5.576
	n	2.013	2.353	2.098
	R^2	0.884	0.977	0.926

As demonstrated by the higher coefficients of determination values (R^2) the equilibrium experimental data were better fitted to Langmuir isotherm model, at all temperature in the studied concentration range of RhB. This means that the adsorption of RhB on OP occurs in monolayer.

Maximum adsorption capacity (Q_m) calculated using Langmuir isotherm model, at temperature values of 278, 295 and 313 K, was found to be 72.8, 95 and 106 mg g^{-1} respectively.

3.5. Comparison with other materials

Compared with some data in the literature (Table 2) it is apparent that olive pomace exhibits a good potential for the removal of RhB aquatic pollutant. However, there is still a need to further investigate and pilot the practical utility of this material on a commercial scale.

Table 2. Maximum adsorption capacity of some adsorbents for RhB

Adsorbents	***Q_m (mg g^{-1})***	***Reference***
Acid treated montmorillonite	188.67	Bhattacharyya et al. (2014)
Raw dika nut waste	212.77	Inyinbor et al. (2015)
Beta zeolites (SiO_2/Al_2O_3)	27.97	Cheng and Liu (2018)
Argemone Mexicana seed	17.29	Khamparia and Jaspal (2016)
Kaolinite	21.65	Bhattacharyya et al. (2014)
Montmorillonite	181.81	Bhattacharyya et al. (2014)
Olive pomace	79.8	Current study

3.6. Adsorption kinetic studies

In this study, the kinetics of adsorption was investigated at 20°C, various pH values (pH 4, pH 6.3 and pH 7) and seven different initial concentrations of RhB (C_0 = 100 to 700 mg L^{-1}). The results obtained for pH 4 and pH 6.3 are very close to those obtained for pH 7 and lead to the same conclusions. To demonstrate that the adsorbent can operate without any chemical addition, only the results obtained under pH 7 are presented below.

The kinetics models of RhB adsorption on the OP were analyzed using pseudo-first order, pseudo-second order, Elovich equation, and intraparticle diffusion models. Data were analyzed using linear regression coefficient of correlation R^2 values. The best fit model has the higher value of R^2. The results for the adsorption of RhB at all the initial concentrations studied are reported in Fig. 5 and Table 3. By analyzing the biosorption dynamic profile of RhB onto OP, presented in Fig. 5, one can divide it in three major stages (i) linear and rapid increase within the first 60 min. This may be due to the availability of a high number of vacant adsorption sites during the preliminary stage of the process. (ii) In the second stage of the process (60-120 min), the rate of the biosorption process get slower. The number of unoccupied sites used for adsorption turn into negligible and consequently the process rate emerges as considerably slower (iii) after about 120 min a plateau regime is reached. The equilibrium is attained, and the adsorption becomes almost constant thereafter.

It can be noted that the values of the coefficient of determination (R^2) of pseudo-second order model, listed in Table 3, range from 0.975 to 0.998. These values are higher than the corresponding values obtained for the first-order model, as well as for all the other models considered here. Besides, the adsorption capacity evaluated from the pseudo-second order model are close to those of the experimental data. This implies that the process of RhB adsorption obeys the pseudo-second order model over the concentration range studied. This would confirm that the rate-limiting step of the RhB biosorption on OP is the chemical adsorption. Therefore, the adsorptive process would involve the formation of chemical bonds between the adsorbent surface and the molecules of the pollutant (Ho and McKay, 1999; Robati, 2013). The same trend was observed, elsewhere, for the adsorption of RhB onto various lignocellulosic biomaterials such as tea waste (Pirbazari et al., 2014), Coconut (Hameed et al., 2008), sunflower seeds (Jóźwiak et al., 2020) and *Azolla pinnata* (Kooh et al., 2016b).

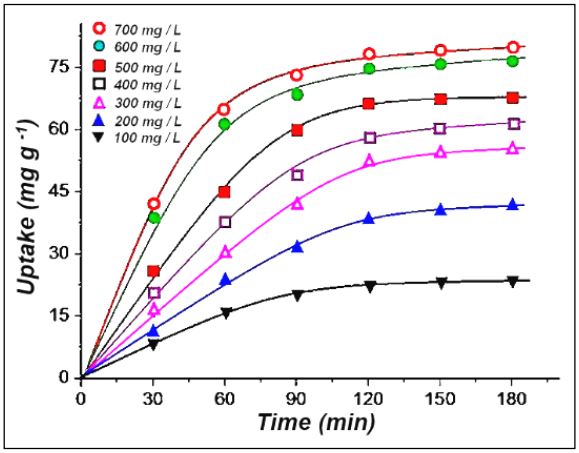

Fig. 5. Effect of contact time and initial dye concentration on RhB removal onto olive pomace (at 293 K and natural initial pH)

The results of the kinetics study indicated that the process obeys the pseudo-second-order model. However, to get more information about the diffusion process of dissolved RhB to the OP surface, further investigations are necessary. Consequently, intraparticle and Elovitch diffusion models were also applied to determine the diffusion model.

The results show that the R^2 values for the intraparticle model are low numbers that are less or equal than 0.96. That may imply that the intraparticle diffusion mechanism does not play a significant role in the RhB adsorption onto the OP. On the other hand, high values of the coefficient of determination for the Elovitch model would confirm that the process of RhB removal is controlled by chemical adsorption.

3.7. FTIR Spectroscopy

Fourier transform infrared spectroscopy (FTIR) is a technique that is sensitive to changes in molecular structure and has been widely used for identification of surface functional groups and their roles in pollutant removal.

Table 3. Kinetic parameters for the biosorption of RhB onto OP

Kinetic models	*Parameters*	*Initial concentration [RhB]$_0$ (mg L^{-1})*						
		100	***200***	***300***	***400***	***500***	***600***	***700***
Pseudo-first order	K_1 (min^{-1})	0.0633	0.052	0.043	0.070	0.098	0.069	0.082
	Q_e (mg g^{-1})	37.5	69.2	264	148	227	135	128.9
	R^2	0.919	0.955	0.848	0.94	0.954	0.953	0.962
Pseudo-second order	K_2	0.0010	0.0004	0.0002	0.0003	0.0003	0.0005	0.0005
	Q_e (mg g^{-1})	32.8	68.8	123.4	119.9	119.8	101.4	104.4
	R^2	0.998	0.995	0.995	0.993	0.985	0.975	0.981
Elovich equation	α	1.057	1.317	1.541	1.909	2.382	4.982	5.210
	β	0.126	0.061	0.041	0.039	0.037	0.043	0.043
	R^2	0.996	0.977	0.977	0.991	0.975	0.956	0.955
Intraparticle diffusion	K_p	1.66	3.52	5.12	5.33	5.39	4.57	4.54
	C	2.98	-3.11	-8.61	-4.66	2.08	24.34	21.55
	R^2	0.941	0.96	0.939	0.935	0.873	0.829	0.846

Fig. 6 and Fig. 7 show the FTIR spectra of OP samples before and after RhB adsorption. The alteration of some of them, carboxyl, amide, and hydroxyl groups, in particular, suggested that these groups are involved in the binding of RhB.

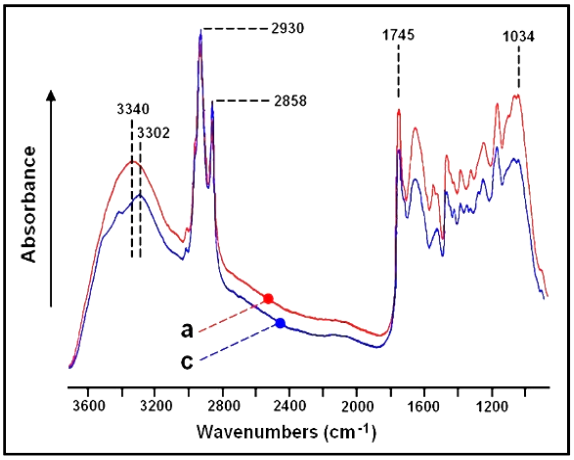

Fig. 6. Combined FTIR spectra of OP before and after RhB adsorption at different RhB initial concentrations: a) before adsorption; c) $[RhB]_0$ = 700 mg L^{-1}

In the 3000−3700 cm^{-1} regions, the band at 3340 cm^{-1} observed in the IR spectrum of OP was due to the –NH_2 groups stretching vibrations (secondary amine) and the stretching vibration of O–H groups. Fig. 6 shows that the intensity of this band at 3340 cm^{-1} decreases with the increase of RhB solution content from 0 to 700 mg L^{-1}. It also could be observed that the band at 3340 cm^{-1} was shifted to 3302 cm^{-1} after loading of RhB. Kooh et al. (2016a) observed such a shift. This can mean that the process of RhB adsorption is accompanied by the consumption of surface amide and hydroxyl groups present on the biomass and that can be an indication that bio-sorption process can occur chemically by some of these active groups (Kooh et al., 2016a).

In the region 1000-1800 cm^{-1}, careful examination of the FTIR spectra for both OP before and after RhB adsorption at different RhB initial concentrations revealed several differences (Fig. 7). One can note that the main peaks and wavenumbers observed for olive pomace are preserved, even though the spectra show significant changes of relative intensities of infrared bands. The weaker intensity of absorbance bands indicates an interaction in the adsorption process (D'Souza et al., 2008; Yapici et al., 2011). In fact, with the increase in initial dye concentration, the intensities of the absorption peaks such as the band at around 1745 cm^{-1} (carboxylic groups), 1650 cm^{-1} (carbonyl groups), 1465 cm^{-1} (bending O–H) decreased gradually after the binding of RhB by the adsorbent. The absorption band at 1540 cm^{-1} (secondary amine group) disappeared after the biosorption of the dye. This is indicative that the carboxyl, the hydroxyl and the secondary amine groups play a significant role in RhB adsorption.

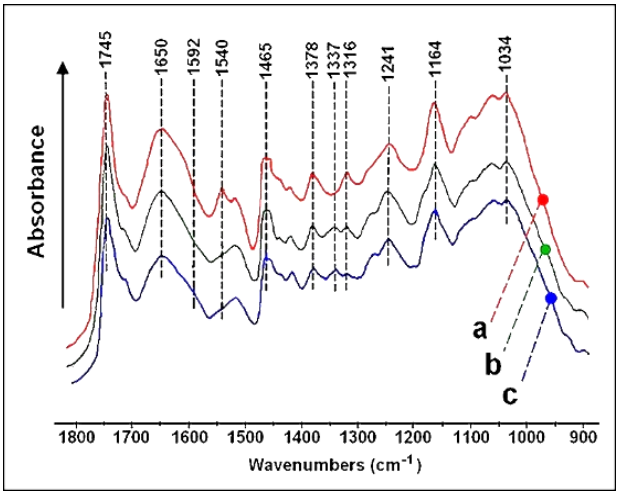

Fig. 7. Combined FTIR spectra of OP before and after RhB adsorption at different RhB initial concentrations: a) before adsorption; b) $[RhB]_0$ = 400 mg L^{-1}; c) $[RhB]_0$ = 700 mg L^{-1}

4. Conclusions

In light of the findings obtained in this study, the following conclusions can be drawn:

1. The sorption equilibrium of RhB is reached after 120 minutes.

2. For the removal of RhB, the optimum pH is found to be 4.

3. Langmuir model best describes the adsorption isotherm of RhB.

4. The pseudo second order model best describes the kinetic of the adsorption.

5. Adsorption of the dye onto the olive pomace is an endothermic proches.

6. Comparison of FTIR spectra of OP before and after RhB adsorption provide direct evidence to show that hydroxyl, carboxyl and amino groups participate in the binding of RhB.

7. Olive Pomace has a good adsorption capacity of RhB and could be used as an innovative green adsorbent for removing the rhodamine B from water.

Acknowledgements

The authors gratefully acknowledge financial support from the Algerian Ministry of Higher Education and Scientific Research.

References

Aboukaïs A., Aouad S., El-Ayadi H., Skaf M., Labaki M., Cousin R., Abi-Aad E., (2012), Physicochemical characterization of Au/CeO_2 solids. Part 2: The impregnation preparation method, *Materials Chemistry and Physics*, **137**, 42-47.

Akar T., Turkyilma S., Celik S., Akar S.T., (2016), Treatment design and characteristics of a biosorptive decolourization process by a green type sorbent, *Journal of Cleaner Production*, **112**, 4844-4853.

Banerjee S., Chattopadhyaya M.C., (2017), Adsorption characteristics for the removal of a toxic dye, tartrazine from aqueous solutions by a low-cost agricultural by-product, *Arabian Journal of Chemistry*, **10**, 1629-1638.

Bharathi K.S., Ramesh S.T., (2013), Removal of dyes using agricultural waste as low-cost adsorbents: a review, *Applied Water Science*, **3**, 773-790.

Bhattacharyya K.G., SenGupta S., Sarma G.K., (2014), Interactions of the dye rhodamine B with kaolinite and montmorillonite in water, *Applied Clay Science*, **99**, 7-17.

Blázquez G., Hernáinz F., Calero M., Martín-Lara M.A., Tenorio G., (2009), The effect of pH on the biosorption of Cr (III) and Cr (VI) with olive stone, *Chemical Engineering Journal*, **148**, 473-479.

Cheng Z.L., Liu Y.L., (2018), Study on adsorption of rhodamine B onto Beta zeolites by tuning SiO_2/Al_2O_3 ratio, *Ecotoxicology and Environmental Safety*, **148**, 585-592.

Crini G., Lichtfouse E., Wilson L., Morin-Crini N., (2019), Conventional and non-conventional adsorbents for wastewater treatment, *Environmental Chemistry Letters*, **17** ,195-213.

D'Souza L., Devi P., Divya Shridhar M.P., Naik C.G., (2008), Use of Fourier Transform Infrared (FTIR) Spectroscopy to study cadmium-induced changes in *Padina tetrastromatica* (Hauck), *Analytical Chemistry Insights*, **3**, 135-143.

EFSA, (2005), Opinion of the Scientific Panel on food additives, flavourings, processing aids and materials in contact with food (AFC) to review the toxicology of a number of dyes illegally present in food in the EU, European Food Safety Authority, *The EFSA Journal*, **263**, 1-71.

Elisee N.B., Dominique R., Carmen M.N., Gerald J.Z., (2018), Determination of point of zero charge of natural organic materials, *Environmental Science and Pollution Research*, **25**, 7823-7833.

Guerrero-Coronilla I., Aranda-Garcia E., Cristiani-Urbina E., (2019), Biosorption of metanil yellow dye from aqueous solutions by the entire water hyacinth plant (*eichhornia crassipes*) and its vegetative organs, *Environmental Engineering and Management Journal*, **18**, 1671-1682.

Hameed B.H., Mahmoud D.K., Ahmad A., (2008), Equilibrium modeling and kinetic studies on the adsorption of basic dye by a low-cost adsorbent: coconut (*Cocos nucifera*) bunch waste, *Journal of Hazardous Materials*, **158**, 65-72.

Ho Y.S., McKay G., (1999), Pseudo-second order model for sorption processes, *Process Biochemistry*, **34**, 451-465.

Hou M.F., Ma C.X., Zhang W.D., Tang X.Y., Fan Y.N., Wan H.F., (2011), Removal of rhodamine B using iron-pillared bentonite, *Journal of Hazardous Materials*, **186**, 1118-1123.

Imam S.S., Babamale H.F., (2020), A short review on the removal of Rhodamine B Dye using agricultural waste-based adsorbents, *Asian Journal of Chemical Sciences*, **7**, 25-37.

Inyinbor A.A., Adekola F.A., Olatunji G.A., (2015), Adsorption of rhodamine B dye from aqueous solution on *Irvingia gabonensis* biomass: kinetics and thermodynamics studies, *South African Journal of Chemistry*, **68**, 115-125.

Inyinbor A.A., Adekola F.A., Olatunji G.A., (2016), Kinetics, isotherms and thermodynamic modeling of liquid phase adsorption of Rhodamine B dye onto Raphia hookerie fruit epicarp, *Water Resources and Industry*, **15**, 14-27.

Isa M.H., Lang L.S., Asaari F.A.H., Aziz H.A., Ramli N.A., Dhas J.P.A., (2007), Low cost removal of disperse dyes from aqueous solution using palm ash, *Dyes and Pigments*, **74**, 446-453.

Jóźwiak T., Filipkowska U., Brym S., Kopeć L., (2020), Use of aminated hulls of sunfower seeds for the removal of anionic dyes from aqueous solutions, *International Journal of Environmental Science and Technology*, **17**, 1211-1224.

Khamparia S., Jaspal D., (2016), Investigation of adsorption of Rhodamine B onto a natural adsorbent *Argemone Mexicana*, *Journal of Environmental Management*, **183**,786-793.

Kooh M.R.R., Dahri M.K. and Lim L.B.L., (2016a), The removal of rhodamine B dye from aqueous solution using *Casuarina equisetifolia* needles as adsorbent, *Cogent Environmental Science*, **2**, 1140553.

Kooh M.R.R., Lim L.B.L., Lim L.L., Dahri M.K., (2016b), Separation of toxic rhodamine B from aqueous solution using an efficient low-cost material, *Azolla pinnata*, by adsorption method, *Environmental Monitoring and Assessment*, **188**, 108-123.

Lima R.O.A., Bazo A.P., Salvadori D.M.F., Rech C.M., Oliveira D.P., Umbuzeiro G.A., (2007), Mutagenic and carcinogenic potential of a textile azo dye processing plant effluent that impacts a drinking water source, *Mutation Research/Genetic Toxicology and Environmental Mutagenesis*, **626**, 53-60.

Martín-Lara M.A., Pagnanelli F., Mainelli S., Calero M., Toro L., (2008), Chemical treatment of olive pomace: effect on acid-basic properties and metalbiosorption capacity, *Journal of Hazardous Materials*, **156**, 448-457.

Martín-Lara M.A., Hernáinz F., Calero C., Blázquez G., Tenorio G., (2009), Surface chemistry evaluation of some solid wastes from olive-oil industry used for lead removal from aqueous solutions, *Biochemical Engineering Journal*, **44**, 151-159.

Nuhoglu Y., Malkoc E., (2009), Thermodynamic and kinetic studies for environmentaly friendly Ni(II) biosorption using waste pomace of olive oil factory, *Bioresource Technology*, **100**, 2375-2380.

Ospina V., Buitrago-Sierra R., López D., (2015), HDO of guaiacol over NiMo catalyst supported on activated carbon derived from castor de-oiled cake, *Ingeniería e Investigación*, **35**, 49-55.

Pagnanelli F., Mainelli S., Veglio F., Toro, L., (2003), Heavy metal removal by olive pomace: Biosorbent characterisation and equilibrium modelling, *Chemical Engineering Science*, **58**, 4709-4717.

Patel H., (2018), Charcoal as an adsorbent for textile wastewater treatment, *Separation Science and Technology*, **53**, 2797-2812.

Pirbazari A.E., Saberikhah E., Badrouh M., Emami M.S., (2014), Alkali treated Foumanat tea waste as an efficient adsorbent for methylene blue adsorption from aqueous solution, *Water Resources and Industry*, **6**, 64-80.

Rizzi V., D'Agostino F., Fini P., Semeraro P., (2017a), An interesting environmental friendly cleanup: The excellent potential of olive pomace for disperse blue adsorption/desorption from wastewater, *Dyes and Pigments*, **140**, 480-490.

Rizzi V., D'Agostino F., Gubitosa J., Fini F., Petrella A., Agostiano A., Semeraro P., Cosma P., (2017b), An alternative use of olive pomace as a wide-ranging bioremediation strategy to adsorb and recover disperse orange and disperse red industrial dyes from wastewater, *Separations*, **4**, 29-41.

Robati D., (2013), Pseudo-second-order kinetic equations for modeling adsorption systems for removal of lead ions using multi-walled carbon nanotube, *Journal of Nanostructure in Chemistry*, **3**, 1-6.

Sergeeva I.P., Sobolev V.D., (2018), The effect of surface charge on adsorption of a cationic polyelectrolyte, *Colloid Journal*, **80**, 86-90.

Srinivasan A., Viraraghavan T., (2010), Decolorization of dye wastewaters by biosorbents: a review, *Journal of environmental management*, **91**, 1915-1929.

Venkatraman B.R., Gayathri U., Elavarasi S., Arivoli S., (2012), Removal of Rhodamine B dye from aqueous solution using the acid activated Cynodon dactylon carbon, *Der Chemica Sinica*, **3**, 99-113.

Yapici S., Eroglu H., Varoglu E., (2011), Bio-sorption of Tl-201 radionuclide on olive pomace, *Applied Radiation and Isotopes*, **69**, 614-622.

Zhao Y., Yang H., Sun J., Zhang Y., Xia S., (2021) Enhanced adsorption of rhodamine B on modified oil-based drill cutting ash: characterization, adsorption kinetics, and adsorption isotherm, *ACS Omega*, **6**, 17086-17094.